



S0008-6223(96)00028-0

EFFECTS OF ACTIVATION METHOD ON THE PORE STRUCTURE OF ACTIVATED CARBONS FROM APRICOT STONES

K. GERGOVA and S. ESER*

Fuel Science Program, Department of Materials Science and Engineering, The Pennsylvania State University, 209 Academic Projects Building, University Park, PA 16802, U.S.A.

(Received 23 May 1995; accepted in revised form 1 February 1996)

Abstract—Two series of activated carbons were prepared from apricot stones by using carbonization followed by steam activation and one-step pyrolysis/activation in steam. The pore structure of the activated carbons was characterized by CO₂ adsorption at 273 K and by N₂ adsorption at 77 K. The macro- and mesoporosity were determined by mercury porosimetry. Optical microscopy, scanning electron microscopy (SEM) and environmental scanning electron microscopy (ESEM) were used to examine the microstructure of activated carbons. A considerable difference observed between the measured CO₂ and N₂ surface areas indicates a narrow microporosity in all the carbons. The two-step method produced better developed meso- and especially macroporosity. The SEM and optical micrographs show that one-step pyrolysis/steam activation preserves the original cell structure of the raw apricot stones. In general, the apparent surface areas of the two-step carbons are slightly higher than those of the one-step carbons. However, the one-step method would provide lower production costs because it would eliminate the separate carbonization stage. Copyright © 1996 Elsevier Science Ltd

Key Words—Activated carbon, apricot stones, pore structure, steam activation, SEM.

1. INTRODUCTION

Both the nature of the precursors and the method of activation have a strong influence on the porous structure and adsorption properties of the resulting activated carbons. Ligninocellulosic materials, such as fruit stones and shells, proved to be excellent precursors for the production of activated carbons. High-quality activated carbons produced from these materials are capable of adsorbing either from gas or liquid phase [1].

Various methods of activation have been used to obtain activated carbons from agricultural waste products. The so-called physical activation includes carbonization of the precursor in an inert atmosphere and activation of the resulting char by CO₂, steam, air or with more than one activation agent [2]. One-step pyrolysis and activation in steam has been used to produce activated carbons from several ligninocellulosic materials, such as apricot and cherry stones, almond, walnut, coconut shells, and grape seeds [3–5]. Almond shells and olive stones as well as plum and peach stones have been used as precursors for the preparation of activated carbons by direct activation in CO₂ [6,7]. The activation with CO₂ is convenient for studying the effects of process conditions on the evolution of the porous structure of carbons, however, a major portion of the commercial activated carbons are produced by steam activation [8].

In this study, we investigate the differences in the porous structure of activated carbons produced from

a single precursor, apricot stones, employing two different methods, a two-step physical activation and one-step pyrolysis/activation. In both cases, steam was used as the activation agent. Apricot stones are abundant waste materials from the canning industry. Their hardness along with the low ash and sulfur contents make them good precursors for activated carbon production.

2. EXPERIMENTAL

California apricot stones from Mayfair Packing Company were used in this study. Apricot stones were crushed and sieved to a particle size of 1–3 mm in diameter. Table 1 shows the proximate and ultimate analyses of the apricot stones. All the values are expressed on a dry basis. One can see that apricot stones have very low sulfur (0.03%) and ash (0.81%) contents. The apricot stones have relatively low carbon (51%) but high oxygen (40%) contents.

Two-step carbons were prepared by carbonization of the precursor in nitrogen at 750–850°C for 2–4 hours followed by activation with steam at 750–950°C for 2–4 hours. One-step carbons were prepared by pyrolysis and partial gasification of the precursor at 600–800°C for 2–3 hours in the presence of steam. The same experimental set-up as described in detail elsewhere [9] was used for producing both series. For carbonization and steam pyrolysis, a 50 g sample of apricot stones was heated in a stainless steel vertical reactor which was placed in a tube furnace. The same heating rate (20°C/min) and steam flow rate (10 g/min) were used for both sets of experiments.

The characterization of the activated carbons was

*To whom correspondence should be addressed.

Table 1. Proximate and ultimate analyses of the apricot stones

Proximate analysis (wt%)				Ultimate analysis (%)				
Moisture	Ash	Volatile	C	H	N	Total S	O by diff.	Ash
5.12	0.81	80.24	51.57	6.34	0.57	0.027	40.68	0.81

carried out by gas adsorption (CO_2 at 273 K and N_2 at 77 K) using a Quantachrome automated adsorption apparatus (Autosorb-1, model ASIT). The adsorption data were analyzed by using the BET equation [11] to calculate the apparent surface areas of the activated carbons and the Dubinin–Radushkevich equation was used to calculate micropore volumes from CO_2 adsorption [12]. The Dubinin–Radushkevich surface areas were determined using the values obtained for the micropore volumes [13]. The total pore volumes were determined from the amount of nitrogen adsorbed at a relative pressure of 0.95. Cross-sectional areas of 0.162 nm² and 0.253 nm² were assumed for N_2 molecules adsorbed at 77 K and for CO_2 molecules adsorbed at 273 K, respectively [14]. The meso- and macroporosity of activated carbons were determined using a Quantachrome Autoscan 60 mercury porosimeter up to a pressure of 60 000 psi for a pore size range of 2–5000 nm.

The microstructures of the activated carbons produced from apricot stones were examined using a polarized-light microscope (Nikon-Microphot-FXA) and a scanning electron microscope (ISI ABT, Model SX-40A). Samples for optical microscopy were mounted in an epoxy resin and polished using alumina. An environmental scanning electron microscope (ESEM) (ES-3 from Electroscan) was also used to observe the microstructural changes of activated carbon precursor during the heating up of the apricot stones to 800°C in the presence of water vapor at 2 torr total pressure. The ESEM enables the direct observation of the surface behavior of unprepared, uncoated samples under controlled atmospheres and temperatures [15,16].

3. RESULTS AND DISCUSSION

3.1 Solid yield and porosity development

Since one-step activation does not include a separate carbonization step, "solid yield" instead of "burn-off" was used to compare the carbons obtained by different activation methods. The solid yield is calculated by dividing the mass of the resulting activated carbon by the initial mass of the precursor apricot stones. Note, that for a fair comparison, the yields reported for two-step carbons are also based on the starting material, and not on the intermediate char.

Comparable char yields and surface areas were obtained from the carbonization of apricot stones at 750–850°C for 2 hours, as shown in Table 2. Based on the surface area measurements on the chars obtained at different temperatures, one can conclude

that the carbonization temperature does not have a significant effect on the pore structure of the resulting chars. For consistency, however, only the chars obtained by carbonization at 750°C for 2 hours were used for activation in the two-step process.

Figure 1 shows the solid yields of one- and two-step carbons obtained after 2 hours of activation as a function of activation temperature. All the chars used for producing two-step carbons were obtained by carbonization at 750°C for 2 hours. For an activation temperature of 750°C, which happens to be the carbonization temperature for two-step carbons, both methods give the same solid yield of approximately 20%. It appears that for activation temperatures higher than 750°C, the solid yields from the two-step operation are higher than those of the one-step.

Table 3 gives the yield and porosity characteristics of the two sets of carbons. The comparison of one- and two-step activated carbons with a similar yield, (i.e. 20.5%, produced at 750°C for 2 hours) shows that the carbon produced in one-step has a considerably higher micro- and mesopore volumes, 0.28 and 0.30 cc/g, respectively, compared to 0.19 and 0.20 cc/g obtained for the two-step carbon. The one-step carbon has, however, a substantially lower macropore volume (0.14 cc/g) compared to that of the two-step carbon (0.28 cc/g). It is important to note that the presence of steam during pyrolysis produces a very different porosity than that generated by steam activation of the previously obtained char at the same temperature.

The activated carbons prepared at 600 and 650°C by the one-step operation and the one produced at 700°C by the two-step process have low pore volumes, due to incomplete pyrolysis and/or low extents of steam activation. To examine the effect of steam on porosity development during pyrolysis at a relatively low temperature, a char sample was prepared at 650°C for 2 hours in N_2 . The yield and porosity characteristics of the 650°C char are also given in Table 3. A comparison of this char with the carbon obtained in one-step at the same activation temperature and time (Table 3) shows that the char has considerably lower weight loss (34.3% yield compared to 24.4% yield for one-step carbon) and its pore volume (0.12 cc/g) is much lower than that of the one-step carbon (0.23 cc/g). Despite the incomplete pyrolysis and low extent of steam activation at 650°C, the presence of steam introduced at the beginning of the pyrolysis of apricot stones leads to a considerable activation of the carbon and decreases the solid yield. These results are in agreement with our previous

Table 2. Solid yield and surface area of char samples obtained from carbonization of apricot stones

Carbonization temperature (°C)	Solid yields (%)	BET N ₂ surface area, (m ² /g)	CO ₂ surface area (m ² /g)
750	26.4	95	145
800	25.8	110	150
850	24.9	140	175

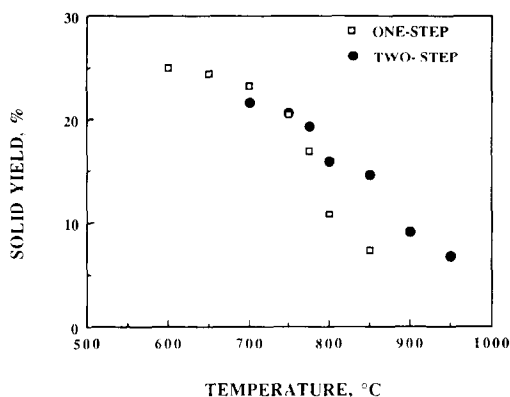


Fig. 1. Solid yield of one- and two-step carbons as a function of temperature.

work on activated carbons from lignite, which shows that water vapor plays an active role in improving the adsorption properties of the resulting solid carbons [17].

Table 3 also shows the total pore volume and micropore volume determined from the CO₂ and N₂ adsorption data using the Dubinin–Radushkevich equation. One can see that the micropore volumes calculated from N₂ and CO₂ adsorption

differ considerably for some carbons. For the carbons with low level of activation (two-step carbon produced at 700°C for 2 hours and one-step carbons produced at 600 and 700°C) the micropore volumes from N₂ adsorption are smaller than or equal to those calculated from the CO₂ adsorption. Most likely, the N₂ adsorption data obtained on these carbons at 77 K do not represent true equilibrium values because of diffusion limitations resulting from narrow microporosity present in these samples. The experimental data do, in fact, show that the adsorption on the carbons is very slow at low relative pressures. For carbons with a low degree of activation, nitrogen molecules cannot enter some of the very fine micropores (up to 0.7 nm) at 77 K because of diffusion limitations (or activated diffusion) and, thus, the adsorption measurements can underestimate the actual microporosity [18,19].

Table 3 shows that the total pore volume and micropore volumes of the two-step carbons increase with the decreasing carbon yield up to 14.5%. Further decrease in the carbon yield decreases the total and micropore volumes of the two-step carbons because of extensive gasification at higher temperatures (>850°C) and/or longer activation times (>2 hours at 800°C). A decrease in the total pore volume and

Table 3. Parameters characterizing the porous structure of activated carbons from apricot stones

Activated carbons				Pore volume (cm ³ /g)			Mercury porosimetry	
Steps	Activation (T°C)	Activation time (h)	Yield (%)	Total pore volume	Micropore volume DR(N ₂)	Micropore volume DR(CO ₂)	Mesopore volume (cm ³ /g)	Macropore volume (cm ³ /g)
2	700	2	21.7	0.28	0.08	0.12	0.18	0.12
2	750	2	20.6	0.36	0.18	0.19	0.20	0.28
2	775	2	19.3	0.37	0.20	0.20	0.23	0.30
2	750	4	16.6	0.48	0.23	0.22	0.32	0.16
2	800	2	15.8	0.52	0.32	0.29	0.38	0.18
2	850	2	14.5	0.55	0.38	0.34	0.40	0.18
2	850	3	13.0	0.54	0.36	0.26	0.35	0.13
2	900	2	9.1	0.44	0.25	0.17	0.19	0.32
2	950	2	6.8	0.33	0.19	0.08	0.12	0.28
1	600	2	25.0	0.22	0.03	0.10	0.15	0.12
1	650	2	24.4	0.23	0.05	0.10	0.20	0.14
1	650	3	24.0	0.25	0.05	0.10	0.22	0.18
1	700	2	23.2	0.28	0.08	0.14	0.28	0.19
1	700	3	21.5	0.29	0.09	0.13	0.30	0.22
1	750	2	20.5	0.50	0.30	0.28	0.30	0.14
1	750	3	18.3	0.62	0.46	0.51	0.23	0.05
1	750	4	16.7	0.70	0.48	0.59	0.24	0.08
1	775	2	16.9	0.53	0.48	0.48	0.25	0.10
1	800	2	10.8	0.61	0.50	0.46	0.32	0.20
1	850	2	7.4	0.37	0.32	0.19	0.36	0.15
char	650-2 hours	—	34.3	0.12	0.04	0.09	0.07	0.02

micropore volume of the one-step carbons begins at a higher solid yield (16.9%) and a lower activation temperature (775°C). The longer activation times between 3 and 4 hours at 750°C considerably increase the total pore volume and micropore volume of the one-step carbons. The highest total pore volume and micropore volume for the two-step series was obtained for the carbon produced by activation at 850°C for 2 hours (0.55 cc/g total pore volume and 0.34 cc/g micropore volume from CO₂ adsorption). In comparison, the highest total and micropore volume for the one-step series was obtained for the carbon produced at 750°C for 4 hours (0.70 cc/g and 0.59 cc/g from CO₂ adsorption, respectively). A longer activation time at 850°C (3 hours) did not improve the pore structure of the two-step carbon.

Differences were observed also in the mesoporosity development in the two sets of samples. The change in the mesoporosity of the two-step carbons follows the same trend as the total pore volume; it increases with the decreasing solid yield up to 14.5% and then begins to decrease with further activation. The mesoporosity of one-step carbons shows a different behavior, however, exhibiting a more varied change with the level of activation. After an initial increase with the decreasing solid yield up to 20.5% solid yield, the mesoporosity decreases slightly with further activation up to 16.7% yield after which it increases again with the decreasing solid yield. It is interesting to note that the large increase in the micropore volume of one-step carbons after 20.5% solid yield coincides with the slight decrease in mesoporosity in the same solid yield range. The subsequent increase in mesoporosity with the decreasing microporosity at high activation levels at 800 and 850°C appears to result from the widening of the micropores because of the extensive gasification at these temperatures. These observations are confirmed by the higher micropore volume obtained from N₂ adsorption compared to that determined by CO₂ adsorption.

No clear trends were observed between the macroporosity of one- and two-step carbons and the solid yields. There is an increase in macroporosity for the carbons produced at high activation temperatures (900–950°C for two-step carbons and 800–850°C for one-step carbons) due to the enlargement of micro- and mesopores and removal of some pore walls.

3.2 Effects of activation temperature and time on porosity development

The data in Table 3 shows that, under the experimental conditions used, both activation temperature and activation time can be used to control the porosity development in one-step carbons. For two-step carbons, however, controlling the porosity by changing the activation time seems to be much more difficult. This different response of the two series to changing activation time can be explained by the vastly different devolatilization/gasification rates in the two processes. A well-developed pore structure is achieved in one-step at a much lower temperature

(750°C) than that for the two-step operation (850°C). At the lower activation temperature of 750°C, the longer activation time will lead to further development of the carbon porosity because the devolatilization/gasification reactions taking place at this temperature are much slower than those at 850°C. At 850°C, the longer activation time leads to extensive gasification and, thus, decreases the porosity of the two-step carbons. As an analogy, one can consider that controlling the evolution of porosity is much more difficult to control during activation with steam than that with CO₂ because of the higher reactivity of solid carbons with steam than with CO₂.

Figure 2 shows the total pore volume (from N₂ adsorption at a relative pressure of 0.95 [11]) as a function of temperature for one- and two-step carbons obtained after 2 hours activation time. There is, in general, a continuous increase in the total pore volume with the increasing activation temperature of the one- and two-step carbons which result from the opening of the initially inaccessible pores. The drastic increase of the porosity between 700 and 800°C can be attributed to high reaction rates of steam with carbon at this temperature. However, the porosity drops sharply after 850°C for two-step carbons and after 800°C for one-step carbons.

Figure 3 compares the total pore volume obtained from 1 g precursor as a function of temperature for one- and two-step carbons. The total pore volume was calculated by multiplication of the volumes of the carbons by the corresponding carbon yield. Since one- and two-step carbons are obtained by different activation methods, it is more reasonable to compare their porosity based on the mass of the precursor. Although, most of the two-step carbons have slightly higher total pore volumes than the one-step carbons, Fig. 3 shows that, based on 1 g precursor, the one-step carbons produced between 700–800°C have comparable or higher porosity. The porosity of one-step carbons as well as the total pore volume/g precursor decreases after 800°C. Generally, developing the porosity of two-step carbons requires higher

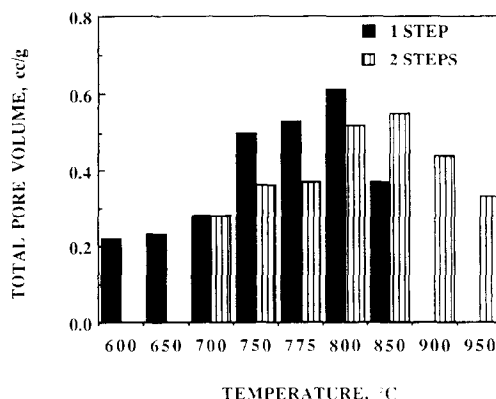


Fig. 2. Total pore volume of one- and two-step carbons as a function of temperature.

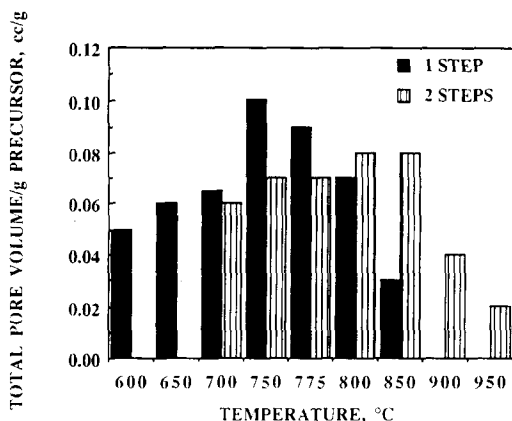


Fig. 3. Total pore volume of one- and two-step carbons from 1 g precursor as a function of temperature.

activation temperature. The same plots can be drawn for the micro-, meso- or macropore volumes of activated carbons from apricot stones in order to compare the effect of different activation methods.

In Fig. 4, the micropore volumes obtained from CO_2 adsorption on one- and two-step carbons are plotted as a function of temperature for a constant activation time of 2 hours. The micropore volumes of two-step carbons followed the same trends as the total pore volumes. The one-step carbons show a continuous increase of the micropore volume up to 775°C . With further increase in the temperature the micropore volume of one-step carbons decreases. These results clearly show that the microporosity of one-step carbons is very sensitive to the changes in activation temperature. In other words, the gasification processes at temperature higher than 775°C starts to decrease the microporosity, while the total and mesopore volumes continue to increase, as expected. The change in microporosity of two-step carbons with temperature is more gradual than that of one-step carbons.

The mercury porosimetry results can give the pore size distribution when $dV/d\log R$ is plotted vs R , where V is the volume of mercury and R is the radius of the pores. Figure 5 shows the pore size distribution

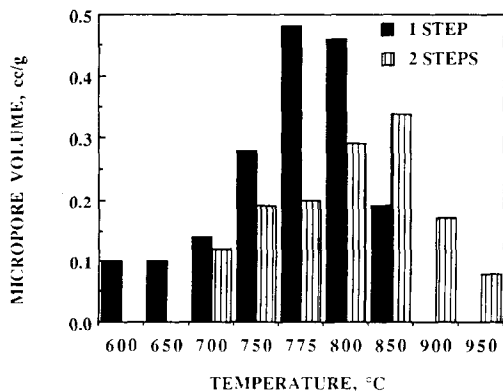


Fig. 4. Micropore volume of one- and two-step carbons as a function of temperature.

curves obtained from mercury porosimetry for activated carbons with the same solid yield (20.5%) produced at 750°C for 2 hours by one- and two-step methods. One can see that the two-step carbon has a bimodal distribution which is not as pronounced in the one-step carbon. In the two-step carbon, one maximum appears in the macropore region at a pore radius of about 800 nm which almost coincides with the maximum of the one-step carbon in the macroporous region. The other maximum of the two-step carbon is in the mesopore region at about 8 nm. One-step carbons have more homogeneous mesopore size distribution and the maximum appears to be wider, about 5–10 nm. This is an indication for external activation of particle surfaces. Because of the higher microporosity of one-step carbons the water molecules cannot penetrate to the interior of the particles which results in developing meso- and macropores on particle surfaces. The presence of meso- and macroporosity in activated carbons produced from apricot stones by one- and two-step process can be useful in adsorption processes since these pores are transportation arteries of adsorbates to microporosity at the interior of the particles.

3.3 Apparent surface areas of activated carbons

Table 4 shows the apparent surface areas of activated carbons and the char sample produced at 650°C for 2 hours determined by N_2 adsorption at 77 K and by CO_2 adsorption at 273 K. The activated carbons in Table 4 are listed in the order of decreasing solid yields. A comparison of N_2 and CO_2 surface areas is a simple indicator of the porosity characteristics of activated carbons. The low N_2 adsorption at 77 K and high CO_2 adsorption at 273 K suggest the presence of narrow microporosity because of low accessibility to N_2 at 77 K. These differences could be used to calculate super-microporosity [20,21]. The apparent surface areas of activated carbons determined by N_2 adsorption are substantially lower than those obtained from CO_2 adsorption for all the carbons. Since the CO_2 molecule is slightly smaller than the N_2 molecule, the activated carbons from

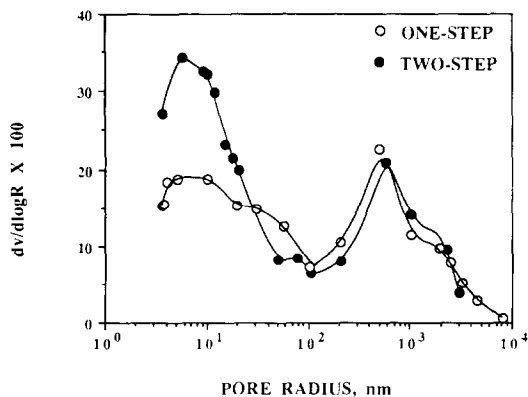


Fig. 5. Pore size distribution curves (mercury porosimetry) of one- and two-step carbon with 20.5% solid yield.

Table 4. Apparent surface areas of activated carbons

Two-step activated carbons				One-step activated carbon porosimetry			
Activation temperature (°C)	Activation time (h)	N ₂ surface area (m ² /g)	CO ₂ surface area (m ² /g)	Activation temperature (°C)	Activation time (h)	N ₂ surface area (m ² /g)	CO ₂ surface area (m ² /g)
700	2	400	940	600	2	380	700
750	2	540	1160	650	2	390	750
775	2	585	1250	650	3	405	850
750	4	600	1190	700	2	450	1000
800	2	620	1120	700	3	500	1050
850	2	900	1030	750	2	670	1100
850	3	750	1020	750	3	810	1190
900	2	715	990	775	2	600	1060
950	2	580	980	750	4	930	1390
Char 650-2 hours	–	45	320	800	2	560	1030
				850	2	520	990

apricot stones should be essentially microporous materials and most of the micropores have slightly larger diameters (up to 0.7 nm) than that of CO₂.

The highest CO₂ surface areas were obtained for activated carbons produced by one-step method at 750°C for 4 hours. One-step carbons with the highest CO₂ surface areas (1190 and 1390 m²/g) were produced by longer activation times (3 and 4 hours) at 750°C. Increasing the activation temperature to 775°C was more effective to obtain a high CO₂ surface area (1250 m²/g) for the two-step carbons. The steam activation at 750°C for 4 hours gives a relatively low CO₂ surface area (1190 m²/g) for the two-step carbon. There is a sharp decrease in the apparent surface areas of the two-step carbons at temperatures higher than 800°C. For one-step carbons, the decrease in surface areas occurs after 750°C. These results are in good agreement with the total pore volumes of activated carbons shown in Table 3. The one-step carbon produced at 750°C for 2 hours, which has the same solid yield as the two-step carbon produced under the same activation conditions, has a higher micropore volume and N₂ surface area and slightly lower CO₂ surface area than the two-step carbon (Tables 2 and 4). These data suggest that the one-step carbon is highly microporous, but there is some broadening of the microporosity compared to the two-step carbon. Nevertheless, the CO₂ surface area of one-step carbon is high (1100 m²/g) and differs considerably from the N₂ surface area, which is evidence that despite some widening of the microporosity, most of the micropores have diameters of 3.5 Å or smaller.

Figures 6 and 7 show the N₂ and CO₂ surface areas, respectively, of one- and two-step carbons plotted as a function of the solid yields. The N₂ and CO₂ surface areas of one-step carbons continuously increase with activation up to 20% solid yield and then begin to decrease. The CO₂ surface areas of one-step carbons decrease more gradually after 20% solid yield while N₂ surface areas drop more quickly. This is an indication that the smallest micropores are removed last during the extensive gasification process. On the other hand, there is a clear maximum in the

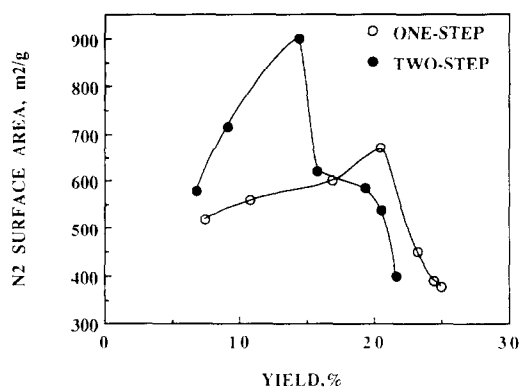


Fig. 6. N₂ surface area of one- and two-step carbon as a function of percentage solid yield.

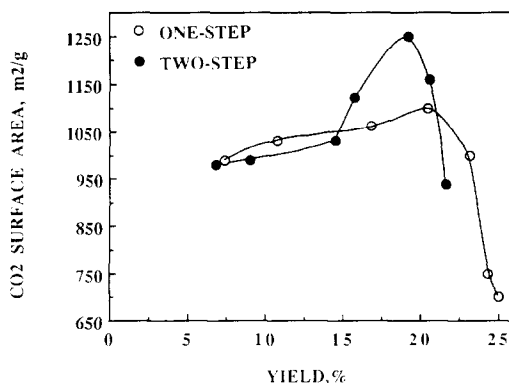


Fig. 7. CO₂ surface area of one- and two-step carbons as a function of percentage solid yields.

plots for the N₂ and CO₂ surface areas of the two-step carbons. The maximum for the N₂ surface area is shifted to lower solid yields. These results suggest that during one-step pyrolysis/activation there is a gradual development of the microporosity of the solid carbon with the increasing extent of activation. A higher extent of activation, which corresponds to the solid yield <20%, leads to widening of already existing micropores and development of meso- and macropores by collapsing some pore walls by gasification.

The development of ultramicropores ($<3.5 \text{ \AA}$) by two-step activation (around 20% solid yield) is followed by widening of the micropores with the increasing activation to develop larger micropores ($>3.5 \text{ \AA}$) around 15% solid yield. The maxima for the N_2 and CO_2 surface areas cover a narrow solid yield range which indicates that controlling the microporosity of the two-step carbons will be difficult.

Figure 8 shows the N_2 adsorption isotherms for selected two-step carbons. Although the N_2 adsorption isotherms are basically of type I, exhibited by microporous solids [22], the shape of the isotherms demonstrates a wider microporosity and the presence of mesoporosity. Type I adsorption isotherms are generally reversible, but microporous materials having mesopores can exhibit hysteresis as a result of capillary condensation in mesopores. Some hysteresis is observed even in the isotherm with the lowest amount adsorbed (9% solid yield) suggesting that a limited mesoporosity is present. The activated carbon with 20% solid yield has the most prominent hysteresis which can be characterized as type A attributed to cylindrical pores [23]. At a high activation degree (9% solid yield), the uptake of nitrogen at a low relative pressure increases, but the isotherm exhibits a more rounded knee, indicating a widening of the micropores.

Figure 9 shows the N_2 adsorption isotherms of selected one-step carbons. The one-step carbon with 25% yield can be considered to have almost ideal type I isotherm. This is an indication that the carbon is almost exclusively microporous with a very narrow microporosity in the range of two molecular dimensions. However, for carbons with 20 and 10% solid yield the isotherms suggest larger micropores and larger adsorption capacity. It should be noted that the one-step carbon with the lowest yield does not correspond to a high porosity which is in agreement with the data in Table 3. If one compares the adsorption isotherms of one- and two-step carbons (although it should be noted that the solid yields are not exactly comparable), the two-step carbons have slightly larger adsorption capacity, larger mesopore volumes (indicated by the hysteresis) and a wider microporosity than those of the one-step carbons.

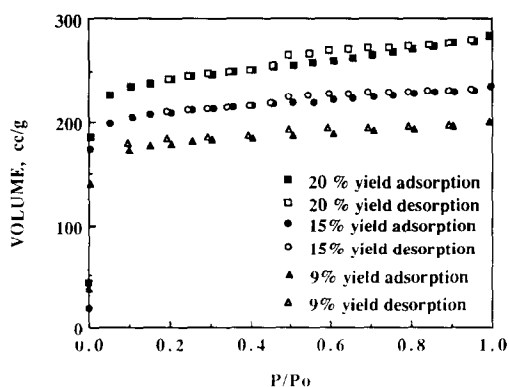


Fig. 8. N_2 adsorption isotherms of selected two-step carbons.

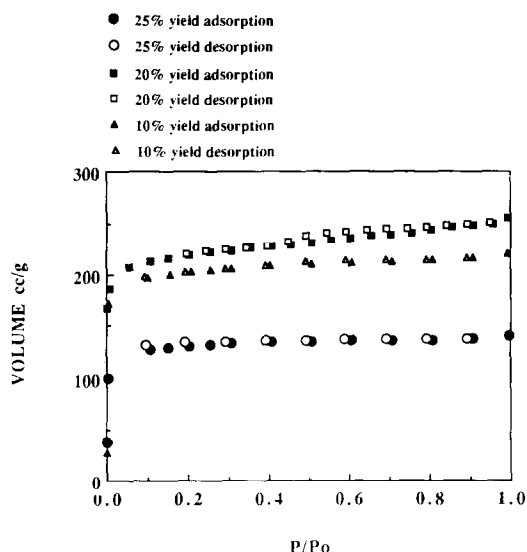


Fig. 9. N_2 adsorption isotherms of selected one-step carbons.

3.4 Microscopic examination of raw material and solid carbons

A microscopic examination of the untreated apricot stones, the char sample and the activated carbons was carried out to better understand the observable porosity development upon carbonization, activation and pyrolysis/activation. The polished surface of the char sample produced by carbonization in N_2 at 750°C for 2 hours and the activated carbons produced by the one- and two-step method at 750°C for 2 hours were examined by optical microscopy using polarized-light.

The surface of char sample (Fig. 10(a)) clearly shows the cell structure of the raw material. There are regions of the micrograph with high concentration of macropores and regions where no pores were observed by optical microscopy. One-step carbon (Fig. 10(c)) shows the same character as the char sample, with regions of highly developed macroporosity and regions with no apparent porosity larger than 500 nm . The sizes of the macropores on the one-step carbon surface are larger than those observed on the char sample presumably because of the gasification reactions with steam. The macropores on the char sample and on the one-step carbon surface have round shapes. The macroporosity on the surface of two-step carbon is well developed (as seen by optical microscopy) and the cell structure of the apricot stones does not appear (Fig. 10(b)). These differences can be seen more clearly in the SEM micrographs.

Some experiments were also performed with ESEM in order to observe the porosity development of apricot stones upon activation with water vapor in real time. Figure 11(a) shows the SEM micrograph of the untreated apricot stones at room temperature. One can see the very specific surface structure of the apricot stones characterized by distinct cells. The surface of the apricot stones is covered with pores which seem to be well arranged. Interestingly, a few

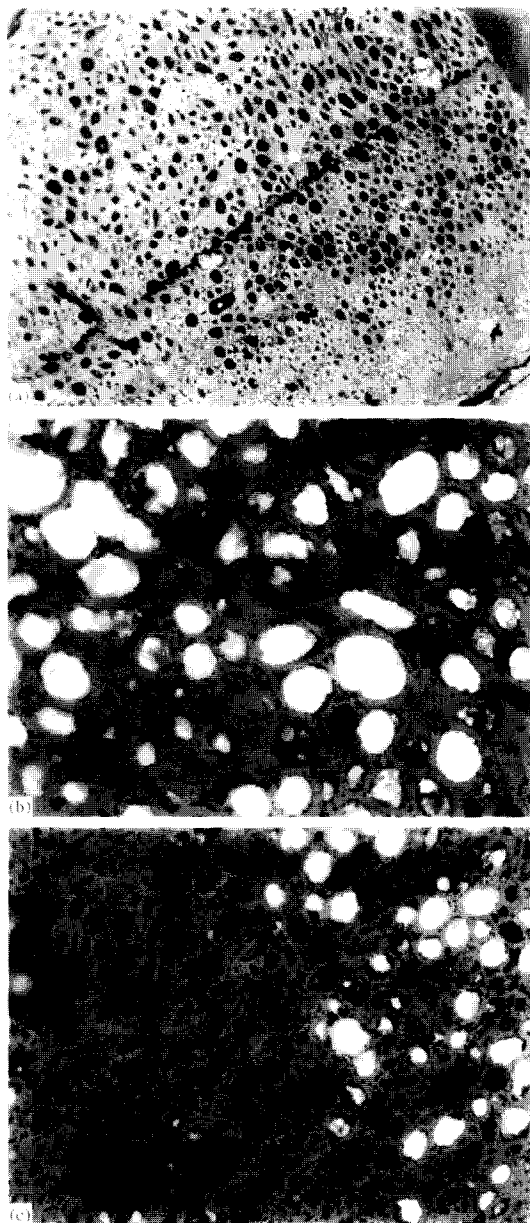


Fig. 10. Polarized-light micrographs of (a) char sample produced at 750°C for 2 h; (b) two-step carbon with 20.5% solid yield, and (c) one-step carbon with 20.5% solid yield. 100 μ m.

very large pits can be clearly seen on the surface of apricot stones located between the cells.

The micrograph in Fig. 11(b) shows the changes in microstructure of apricot stones after treatment for 3 hours during isothermal holding at 800°C in water vapor. The original cell structure is completely preserved and some of the pores on the surface have been enlarged. The micrograph in Fig. 11(b) suggests that the large pores on the surface are connected with a whole network of smaller pores in the interior of the carbon.

Figure 12(a–c) shows the regular scanning electron micrographs of the char sample (a), two-step carbon

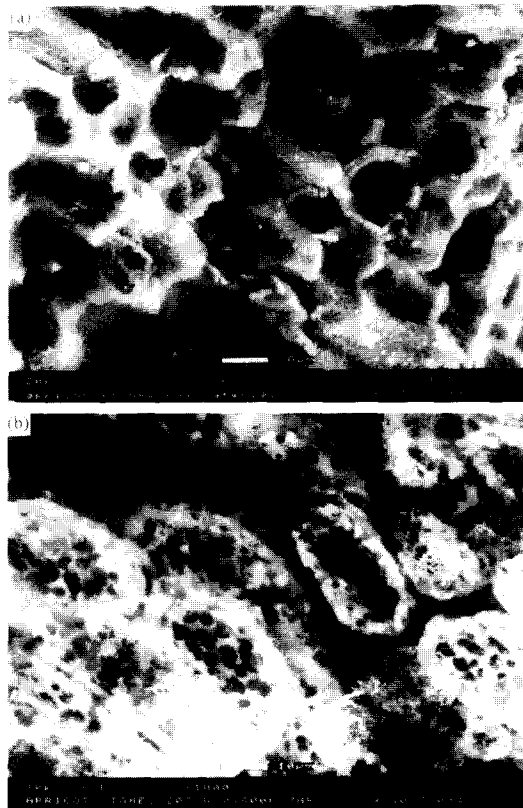


Fig. 11. Environmental scanning electron micrographs of (a) untreated apricot stones; (b) apricot stones heated in water vapor atmosphere at 800°C for 3 hours.

(b) and one-step carbon (c) with the same solid yield (20.5%). The two-step carbon (b) has a more developed macroporosity than the one-step carbon (c). The macropores with oblong shapes in the two-step carbon (b) resulted most probably from the coalescence of two neighboring pores. It seems that in the macropore structure of the two-step carbon all the pores are connected by smaller pores, forming a large network which can be seen on the carbon surface. One-step carbons, on the other hand, have a completely different appearance which resembles the surface of the char produced in the two-step method. It appears that the activation stage in the two-step method substantially changes the char morphology (as seen by SEM). During the carbonization of apricot stones the volatile matter produces a high pressure which breaks the cellular structure of the particles and forms a new structure characterized by deep pores seen on the surface of the char and one-step carbon as well as on the surface of the carbon treated in water vapor at 800°C for 3 hours by ESEM (Fig. 11(b)). However, the presence of steam during pyrolysis in the one-step method also produces fine porosity and preserves the apparent char morphology.

The shape of the pores which can be observed by SEM are also rather different. The gases released on thermal decomposition during one-step

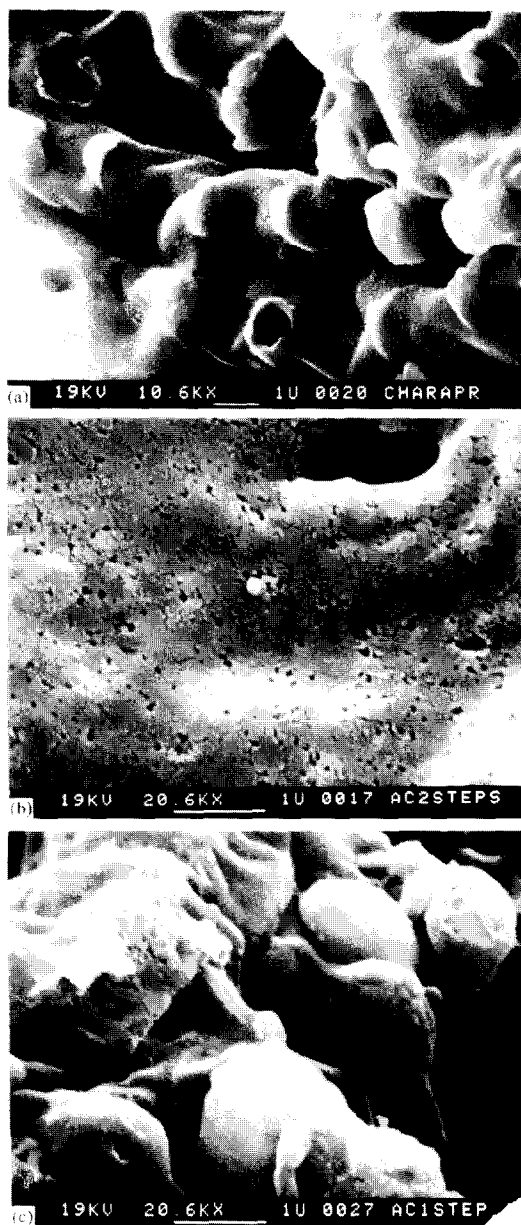


Fig. 12. Scanning electron micrographs of (a) char sample produced at 750°C for 2 hours; (b) two-step carbon with 20.5% solid yield; (c) one-step carbon with 20.5% solid yield.

pyrolysis/activation created hollows in the carbon particles from which they escape through small channels and created bottle-shaped pores. In the case of the two-step process, during activation of carbonized apricot stones by steam there is a water vapor concentration gradient between the entrance and the center of the pores and the oxidation process occurs at a higher rate close to the pore entrances than in the pore centers. This is more likely the reason for creating the pores with conical shape [2].

4. CONCLUSIONS

The steam activation of apricot stones produces carbons with well-developed porosity and surface

area. An activation temperature lower than 700°C for one-step carbons and 750°C for two-step carbons produces activated carbon with incomplete porosity development because of low extent of steam activation. However, an activation temperature higher than 750°C for one-step carbons and 800°C for two-step carbons leads to enlargement of the micro- and mesopores and a decrease in the apparent surface area. In order to achieve good porosity development and high surface area, one should use relatively low temperature and long reaction time for one-step carbons and higher temperatures and shorter activation times for two-step carbons.

The CO₂ surface areas measured at 273 K are considerably higher than the N₂ surface areas measured at 77 K for all the activated carbons. These results suggest the presence of narrow micropores which are not accessible to N₂ molecules especially at this low temperature (77 K). Some diffusion problems have been observed during the nitrogen adsorption which was slow at the low relative pressures. The activated carbons from apricot stones produced by the one- and two-step method have rather wide pore size distribution with well developed microporosity. The mercury porosimetry measurements show the presence of some meso- and macropores.

Although the N₂ as well as the CO₂ surface areas of two-step carbons have slightly higher values than those of one-step carbons, the comparison of the carbons with the same product yield shows that the carbons produced by one-step activation have higher micro- and mesoporosity and lower macroporosity than those produced by the two-step process. The microstructures of the one- and two-step carbons, as observed by optical and SEM are very different, clearly demonstrating the effect of activation method used. The microstructures of the two-step carbons suggests layer by layer activation with the presence of macropores on the surface of activated carbons connected with a large network of meso- and micropores running to the interior of the carbon particles. On the other hand, the one-step pyrolysis/steam activation leads to preservation of the apparent original cell structure of apricot stones. The SEM observations of the carbon surfaces suggested that the shape of the pores of one-step carbons is predominantly round and bottle shaped while two-step carbons are likely to have conical shaped pores.

Combining the two-stages of carbonization and activation into a single step appears to be preferable to two-step treatment because of the lower activation temperature used which would save both energy and time, especially by the elimination of the carbonization step. [10]

REFERENCES

1. J. S. Mattson and H. B. Mark, Jr. *Activated Carbon Surface Chemistry and Adsorption from Solution*. Marcel Dekker Inc., New York (1971).
2. R. C. Bansal, J. B. Donnet and F. Stoeckli, *Active Carbon*. Marcel Dekker Inc., New York (1988).

3. K. Gergova, A. N. Galushko, N. Petrov and V. Minkova, *Carbon* **30**, 72 (1992).
4. K. Gergova, N. Petrov and V. Minkova, *J. Chem. Techn. and Biotechnol.* **56**, 77 (1993).
5. K. Gergova, N. Petrov, L. Butuzova, V. Minkova and L. Isaeva, *J. Chem. Techn. and Biotechn.* **58**, 321 (1993).
6. F. Rodriguez-Reinoso, A. Linares-Solano, M. Molina-Sabio and J. Lopez-Gonzalez, *Ads. Science and Technology* **1**, 211 (1984).
7. F. Rodriguez-Reinoso, J. Martin-Martinez, M. Molina-Sabio, J. Perez-Lledo and C. Prado-Burgete, *Carbon* **23**, 19 (1985).
8. C. Pierce and R. N. Smith, *J. Phys. Chem.* **57**, 64 (1953).
9. F. Rodriguez-Reinoso and M. Molina-Sabio, *Carbon* **30**, 1111 (1992).
10. V. Minkova, M. Razvigorova, M. Goranova, L. Ljutzkanov and G. Angelova, *Fuel* **70**, 713 (1991).
11. S. J. Gregg and K. S. W. Sing, *Adsorption, Surface Area and Porosity*, p. 85. Academic Press, London (1982).
12. M. M. Dubinin and L. V. Radushkevich, *Dokl. Akad. Nauk, SSSR* **55**, 331 (1947).
13. M. Iley, H. Marsh and F. Rodriguez-Reinoso, *Carbon* **11**, 633 (1973).
14. J. R. Tyler and H. J. Wouterlood, *Carbon* **9**, 467 (1971).
15. N. Boumgarten, *Nature* **341**, 81 (1981).
16. K. Gergova, S. Eser, H. H. Schobert, M. Klimkiewicz and P. W. Brown, Environmental Scanning Electron Microscopy of Producing Activated Carbons from Anthracite Using One-Step Pyrolysis/Activation *Fuel* **74**, 1042 (1995).
17. N. Petrov, K. Gergova and S. Eser, *Fuel* **73**, 7, 1197 (1994).
18. P. Ehrburger, N. Pusset and P. Dziedzic, *Carbon* **30**, 1105 (1992).
19. F. Rodriguez-Reinoso, J. Carrido, J. M. Martin-Martinez, M. Molina-Sabio and R. Torregrosa, *Carbon* **27**, 23 (1989).
20. P. L. Walker, Jr, L. G. Austin and S. P. Nandi, In *Chemistry and Physics of Carbon*, pp. 257–371. Marcel Dekker, Vd. 2, (1966).
21. M. J. Illan-Gomez, A. Linares-Solano, C. Salinas-Martinez de Lecea and J. M. Carlo, *Energy and Fuels* **7**, 146 (1993).
22. S. Brunauer, L. S. Denning, W. S. Denning and E. Teller, *J. Am. Chem. Soc.* **62**, 1723 (1940).
23. J. H. de Boer, *The Structure and Properties of Porous Materials*, p. 68. Butterworths, London (1958).